Available online at http://scik.org

Commun. Math. Biol. Neurosci. 2020, 2020:49

https://doi.org/10.28919/cmbn/4779

ISSN: 2052-2541

COST-EFFECTIVENESS AND BACKWARD BIFURCATION ANALYSIS ON COVID-19 TRANSMISSION MODEL CONSIDERING DIRECT AND INDIRECT TRANSMISSION

DIPO ALDILA*

Department of Mathematics, Universitas Indonesia, Depok 16424, Indonesia

Abstract: Since it was first discovered in Wuhan, China, COVID-19 has continued to spread throughout the world. Since then, many research works have been conducted to understand the spread of COVID-19. In this article, we propose an epidemiological model to understand the spread of COVID-19, considering the saturated treatment rate, direct/indirect transmission, and optimal control problem to find the best strategy for the COVID-19 eradication program. The model constructed is based on a nonlinear system of ordinary differential equations. Analytical results regarding the basic reproduction number and all equilibrium points are obtained analytically. Our model shows a possibility of the existence of the COVID-19 endemic state such that even the basic reproduction number is less than unity. We also found that indirect transmission contributes to the increases in the basic reproduction number and also the occurrence of the multiple endemic states. An optimal control approach was applied to determine the best strategy for the COVID-19 eradication program. Three control parameters were considered in the model: medical mask, disinfectant, and medical treatment. A Pontryagin's Maximum Principle was used to derive the optimal control characterization of the related model and was solved numerically using the forward-backward iterative method.

*Corresponding author

E-mail address: aldiladipo@sci.ui.ac.id

Received June 18, 2020

Several simulations were conducted to determine the impact of interventions for short time experiments. From the cost-effectiveness analysis, we found that using a medical mask as a single intervention is the most effective strategy to reduce the spread of infection.

Keywords: COVID-19; direct-indirect transmission; basic reproduction number; medical mask; disinfectant; treatment; optimal control; cost-effectiveness.

2010 AMS Subject Classification: 00A69, 37N25, 93D20.

1. INTRODUCTION

At the end of 2019, the world was shocked by the discovery of a new variant of the coronavirus known as the COVID-19 [1]. The strongest suspicion is that the virus was first spread through animals and then transmitted to humans. Since it was first discovered in the animal market in Wuhan, China, the disease has continued to spread throughout the world. According to data from WHO until 15 July 2020, more than 13 million cases have been detected worldwide. From the total cases, only about 8 million cases ended in recovery, while the other 586,821 cases resulted in deaths. With a Case Fatality Rate (CFR) value of only 7 %, COVID-19 is not categorized as deadly as a MERS disease which has a CFR value of 34%.

There is an early report's advice that transmission might occur from three paths [2] i.e., (1) contact with an object that has the virus on it; (2) inhaling droplets emitted by sneeze and coughs; (3) *micro-droplet* infection. This third infection path is suspected to have resulted from a close contact (conversation or even from standing at a certain distance apart) with infected individuals. In the experiment from NHK, it was found that when an infected individual coughs in a closed space, it is estimated that about a hundred thousand droplets are released within a few seconds. Compared to *large droplets* that fall to the floor within 20–30 seconds, *micro-droplets* remain in the air for a longer period. This leaves people at risk of infection virtually all the time.

Several interventions have been put in place by the government to control the spread of COVID-19 such as (1) endemic prevention strategy (mitigation strategy) and (2) endemic reduction strategy (suppression strategy). This first strategy focused on slowing the spread of COVID-19 such as combining home isolation of suspect cases, social distancing, and so on. The second strategy aims to reverse the growth of COVID-19 through the improvement of medical treatment policy, research on medicine and vaccine for COVID-19, and so on [3]. These strategies

have their own challenges whether it is from human behavior, minimum funding for prevention/control strategy, and so on.

Since COVID-19 was declared by WHO as a global pandemic, there have been many mathematical models introduced by authors to understand how COVID-19 spreads with the help of many aspects such as a model to understand the impact of non-pharmaceutical interventions (NPIs) [3], a model for understanding the effect of undetected cases [4,5], and a model for parameter estimation [6,7,8]. In this article, the result objective is focused on understanding the effect of micro-droplet transmission and its contribution to COVID-19 spread. Many reports have stated that medical resources are very limited in many countries. Therefore, we have included a saturated treatment rate in our model. The model is constructed with a basic SIS model combined with a new compartment for the droplets. Mathematical analysis regarding the stability analysis of the equilibrium points and the existence of backward bifurcation was conducted rigorously. For practical purposes for the COVID-19 control program, we constructed an optimal control problem based on our proposed model by adding three types of intervention as a time-dependent parameter: medical mask use, disinfectant intervention, and medical treatment. An optimal control problem analysis was conducted to determine the best strategy to reduce the number of COVID-19 infected individuals with an optimal intervention, which will depend on time. Some numerical experiments were conducted to provide a visual interpretation of the analytical results.

The rest of the paper is organized as follows. We propose our COVID-19 transmission models in Section 2. The first model is proposed without any intervention implemented. The purpose is to analyze the possible intervention strategy that might be implemented for COVID-19 prevention and endemic reduction purposes. The second model is proposed for policy purposes to eradicate COVID-19. In Section 3, optimal control simulations are conducted based on the second model. Discussion on the cost-effectiveness analysis provided in Section 4, and followed with some conclusions in Section 5.

2. MATERIAL AND METHODS

2.1 Model without control program

2.1.1 Model formulation

To study the effect of indirect transmission and limited medical resources on the spread of COVID-19, in this section, we present the formulation of the model that will examine the dynamics of COVID-19. Human population $(N(t))$ is divided into two compartments: susceptible $(S(t))$ and infected $(I(t))$ compartments. The model is based on the standard SIS model. As mentioned previously, the droplet produced by an infected human through cough or sneeze can last a long time on surfaces [9]. Therefore, it is important to accommodate the existence of the droplets that are free in the environment which, in this article, we denote with $(V(t))$.

Let the recruitment with the constant rate given by A always be susceptible. The susceptible population is decreased by infection with an infected population following a population dependent infection function. This infection parameter is formed by a multiplication between the average number of meetings between S and I for each time interval Δt denoted as c_h, and the chance of success infection denoted as η_h. Therefore, the infection caused by direct contact between susceptible and infected individual is given by $c_h\eta_h\frac{S}{S+I}I$, where $\frac{S}{S+I}$ is the proportion of the susceptible population in time t. For simplification, we wrote $c_h\eta_h = \beta_h$. In addition to direct infection, we assumed that COVID-19 can also be transmitted to susceptible humans S through contact between healthy human and surfaces containing the coronavirus V. Unlike the previous direct infection, the indirect infection in this article is assumed to be modeled as a mass contact between the healthy population and coronavirus on the surface with an infection rate of β_v. Therefore, indirect transmission of Covid-19 is given by $\beta_v S\,V$.

Next, it is important to mention other details on the recovery rate in this article. In many countries, medical resources significantly impact the success of COVID-19 control policy. Unfortunately, the medical resources to control COVID-19 are limited in terms of the number of medical personnel, the availability of hospital beds, and many other factors. To accommodate this situation, the recovery rate that transfers the infected population into the susceptible population is in the term of $\frac{\alpha}{1+bI}$, where α and b are the recovery rate and half saturated parameter, respectively.

Based on this explanation, we formulate the transmission model for COVID-19 with the direct and indirect transmission as well as saturated treatment as follows:

$$\begin{aligned}\frac{dS}{dt} &= A - \frac{\beta_h SI}{S+I} - \beta_v S\,V - \mu_h S + \frac{\alpha I}{1+bI},\\ \frac{dI}{dt} &= \frac{\beta_h SI}{S+I} + \beta_v S\,V - \mu_h I - \frac{\alpha I}{1+bI} - \mu_c I,\\ \frac{dV}{dt} &= \xi I - \mu_v V,\end{aligned} \tag{1}$$

where μ_c is the death rate induced by disease, ξ is the average of production of coronavirus from the infected individual, and μ_v is the expected rate of survival of the coronavirus in the environment. System (1) is supplemented with a non-negative initial condition

$$S(t=0) = S_0 \geq 0, I(t=0) = I_0 \geq 0, V(t=0) = V_0 \geq 0.$$

The rate of change on the total of human populations is as follows:

$$\frac{dN}{dt} = A - \mu_h N - \mu_c I.$$

As we assume that $A = \mu_h N$, therefore we have the total of human population decreasing with respect to COVID-19 death incidence. It is easy to see that $N(t)$ for all $t > 0$, and $N(t) \in \left[0, \frac{A}{\mu_h}\right]$ for $t \to \infty$. Since $\frac{dV}{dt}(V=0) = \xi I$, we have that $V(t)$ always non-negative and has the upper bound $\frac{\xi A}{\mu_h \mu_v}$. Therefore, we have $V(t) \in \left[0, \frac{\xi A}{\mu_h \mu_v}\right]$ for all time $t > 0$. With these properties, we have that system (1) is a biologically well-posed problem.

2.1.2 Model analysis

Before we analyze the model, it is important to reduce the model into a two-dimensional system, using the fact that V has a very fast dynamic as the survival rate μ_v is much larger than the human survival rate μ_h, that is $\mu_v \gg \mu_h$. Using the Quasi-Steady-State Approximation (QSSA) approach [10] and taking V in the equilibrium state, we have $V^* = \frac{\xi I}{\mu_v}$. Substituting V^* into $\frac{dS}{dt}$ and $\frac{dI}{dt}$ on system (1), we have the new COVID-19 model:

$$\begin{aligned}\frac{dS}{dt} &= A - \frac{\beta_h SI}{S+I} - \beta_v S\,\frac{\xi I}{\mu_v} - \mu_h S + \frac{\alpha I}{1+bI},\\ \frac{dI}{dt} &= \frac{\beta_h SI}{S+I} + \beta_v S\,\frac{\xi I}{\mu_v} - \mu_h I - \frac{\alpha I}{1+bI} - \mu_c I.\end{aligned} \tag{2}$$

The next step is re-scaling the time-space into recovery rate time-space by using $\tau = t/\alpha$, where τ is the new time-space. Thus, equation (2) is now read as follows:

$$\begin{aligned}\frac{dS}{d\tau} &= A^* - \frac{\beta_h^* SI}{S+I} - \beta_v^* SI - \mu_h^* S + \frac{I}{1+bI},\\ \frac{dI}{dt} &= \frac{\beta_h^* SI}{S+I} + \beta_v^* SI - \mu_h^* I - \frac{I}{1+bI},\end{aligned} \tag{3}$$

where $A^* = \frac{A}{\alpha}, \beta_h^* = \frac{\beta_h}{\alpha}, \beta_v^* = \frac{\beta_v \xi}{\mu_v \alpha}, \mu_h^* = \frac{\mu_h}{\alpha}$, and $\mu_c^* = \frac{\mu_c}{\alpha}$. Using these assumptions, all parameters now have no dimension except b which is $\frac{1}{individual}$. For the sake of written simplification, we neglect the "*" sign in all parameters and read system(3) as follows:

$$\begin{aligned}\frac{dS}{d\tau} &= A - \frac{\beta_h SI}{S+I} - \beta_v SI - \mu_h S + \frac{I}{1+bI},\\ \frac{dI}{dt} &= \frac{\beta_h SI}{S+I} + \beta_v SI - \mu_h I - \frac{I}{1+bI} - \mu_c I.\end{aligned} \tag{4}$$

One of the most important concepts in analyzing the epidemiological model of disease is the concept of the basic reproduction number which is commonly denoted as R_0. The basic reproduction number has been used by many authors to determine the behavior of the stability of the equilibrium from their disease model [11–15]. Commonly, the disease will die out whenever $R_0 < 1$ and persist whenever $R_0 > 1$. In this section, we will derive the basic reproduction number as the spectral radius of the next-generation matrix of the disease model. Please see [16] for further detail on the next-generation matrix approach in determining R_0 and [17–20] for more examples of the implementation of this method in some epidemiological models.

System (4) always has a trivial equilibrium state, that is, a COVID-19 free state which given by

$$\Gamma_0 = (S, I) = \left(\frac{A}{\mu_h}, 0\right).$$

Applying the next-generation matrix approach to system (4), the basic reproduction number of system (4) is given by

$$R_0 = \frac{A\,\beta_v + \beta_h \mu_h}{\mu_h(\mu_h + \mu_c + 1)}. \tag{5}$$

Theorem 1. *System (4) has a COVID-19 free state Γ_0, which is locally asymptotically stable if $R_0 < 1$ and unstable if $R_0 > 1$.*

Proof. Linearize system (4) at Γ_0 yield

$$J_0 = \begin{bmatrix} -\mu_h & 1 - \beta_h - \frac{\beta_v A}{\mu_h} \\ 0 & \beta_h - 1 + \frac{\beta_v A}{\mu_h} - \mu_h - \mu_c \end{bmatrix}.$$

The eigenvalues of J_0 are $\lambda_1 = -\mu_h$ and $\lambda_2 = (1 + \mu_h + \mu_c)(R_0 - 1)$. Therefore, it is clear that all eigenvalues of J_0 will be negative if $R_0 < 1$. Hence, Γ_0 is locally asymptotically stable if $R_0 < 1$. On the other hand, if $R_0 > 1$, then Γ_0 will be a saddle point. Hence, the proof is complete. ■

From the form of the basic reproduction number, when $\beta_v = 0$, which indicate that we neglect the indirect transmission, we have

$$R_0^* = \frac{\beta_h}{(\mu_h + \mu_c + 1)} < R_0.$$

Remark 1. *The indirect transmission that occurs from contact with objects containing viruses on their surface will increase the standard basic reproduction number from direct contact transmission only. Therefore, using disinfectant to kill the coronavirus could be a wise option to reduce the transmission of COVID-19 in the community.*

Next, we analyze the existence of the untrivial equilibrium point. Taking the right-hand side of system (4) equal to zero and solving it with respect to S and I, the endemic state of system (4) is given by

$$\Gamma_1 = (S, I) = (S^1, I^1),$$

where $S^1 = \frac{c_2 I^2 + c_1 I + c_0}{d_2 I^2 + d_1 I + d_0}$, $c_2 = b\,\beta_v(\mu_c + \mu_h)$, $c_1 = (\beta_v + b\mu_h)(\mu_h + \mu_c) - b\,\beta_v A$, $c_0 = \mu_h(\mu_h + \mu_c + 1) - A\,\beta_v$, $d_2 = -b\,\beta_v(\mu_c + \mu_h)$, $d_1 = b\,(\beta_v A + \beta_h \mu_h) - (\mu_c + \mu_h)(b\mu_v + \beta_v)$ and $d_0 = \mu_h(\mu_c + \mu_h + 1)(R_0 - 1)$, while I^1 is taken from the positive roots of the following polynomial:

$$F(I) = a_3 I^3 + a_2 I^2 + a_1 I + a_0 = 0,$$

Where

$a_0 = A\,\mu_h(\mu_h + mu_c + 1)(R_0 - 1)$,

$a_1 = A\,(A\,\beta_v + \mu_h(\beta_h - \mu_c - \mu_h))b - \beta_h\mu_h(\mu_c - \mu_h) + \beta_h\mu_h(\mu_c + \mu_h) + \mu_h\mu_c(1 + \mu_h + \mu_c)$,

$a_3 = b\,\beta_v\mu_c(\mu_c + \mu_h)$,

while a_2 has an expression too long to be shown in this article.

To analyze the existence of a positive solution of polynomial $F(I)$, we will analyze the sign of $\frac{\partial I}{\partial R_0}$ at $I = 0, R_0 = 1$. If $\frac{\partial I}{\partial R_0} < 0$ at $I = 0, R_0 = 1$, then we will have an endemic equilibrium when $R_0 < 1$ which indicates the existence of backward bifurcation. To do this, we should express all coefficient of $F(I)$ in the term of R_0. To do this, we choose β_h as the bifurcation parameter and solve R_0 respect to β_h which gave us

$$\beta_h^* = \frac{R_0\mu_h(\mu_h + \mu_c + 1) - \beta_v A}{\mu_h}.$$

Substituting $\beta_h = \beta_h^*$ into $F(I)$, we have

$$F^*(I) = a_3^* I^3 + a_2^* I^2 + a_1^* I + a_0^* = 0,$$

where a_3^*, a_2^*, a_1^* and a_0^* now is a function of R_0. Taking the derivative of I respect to R_0 from $F^*(I)$, and then solve it respect to $\frac{\partial I}{\partial R_0}$ at $I = 0, R_0 = 1$ yield

$$\frac{\partial I}{\partial R_0}(I = 0, R_0 = 1) = -\frac{A(\mu_h + \mu_c + 1)}{Ab\mu_h - A\beta_v\mu_c - \mu_h^2(\mu_h + \mu_c + 1)}.$$

It can be seen that $\frac{\partial I}{\partial R_0}$ at $I = 0, R_0 = 1$ will be negative if

$$b > b^\dagger = \frac{A\beta_v\mu_c + \mu_h^2(\mu_c + \mu_h + 1)}{A\,\mu_h}.$$

Therefore, we can conclude that whenever $b > b^\dagger$, there will always exist an endemic state of COVID-19 of system (4) when $R_0 < 1$. This result is summarized in the following theorem.

Theorem 2. *System (4) will have a positive endemic state when $R_0 < 1$ if $b > b^\dagger$, where $b^\dagger$ is given by*

$$b^\dagger = \frac{A\beta_v\mu_c + \mu_h^2(\mu_c + \mu_h + 1)}{A\,\mu_h}.$$

Theorem 2 states the existence of the COVID-19 endemic state even though $R_0 < 1$. In the following theorem, we state the stability criteria of the COVID-19 equilibrium state.

Theorem 3. *System (4) undergoes a backward bifurcation at $R_0 = 1$ if $b > b^\dagger$, where $b^\dagger$ is given in Theorem 2.*

Proof. To analyze the stability of the COVID-19 endemic state, we will use the Castillo-Song theorem which introduced in [27]. First, let system (4) be redefined as follows

$$f_1 := A - \frac{\beta_h SI}{S+I} - \beta_v SI - \mu_h S + \frac{I}{1+bI},$$
$$f_2 := \frac{\beta_h SI}{S+I} + \beta_v SI - \mu_h I - \frac{I}{1+bI}.$$

Next, let β_h be the bifurcation parameter. Hence, β_h is evaluated when $R_0 = 1$.

$$\beta_h^* = \frac{\mu_h(\mu_h + \mu_c + 1) - \beta_v A}{\mu_h}.$$

Substituting $\beta_h^*, \Gamma_0 = \left(\frac{A}{\mu_h}, 0\right)$ into the Jacobian matrix of our system and evaluating the eigenvalues with respect to it, we have one zero simple eigenvalue, and the other eigenvalue is $-\mu_h$. Hence, we can use the center-manifold theorem to analyze the stability of Γ_1.

To use the Castillo-Song theorem, first, we need to calculate the left and right eigenvectors related to the zero eigenvalue. Using a simple calculation, we have the right eigenvector of our system with respect to $\lambda = 0$ is $[w_1 \quad w_2]^T$, where $w_1 = \frac{-(\mu_c + \mu_h)w_2}{\mu_h}, w_2 = w_2$. On the other hand, the left eigenvector with respect to $\lambda = 0$ is $[v_1 \quad v_2]$, where $v_1 = 0, v_2 = v_2$. Since $v_1 = 0,$ we only need to calculate the second partial derivative of f_2 as follows:

$$\frac{\partial^2 f_2}{\partial S^2} = 0, \frac{\partial^2 f_2}{\partial S \partial I} = \frac{\partial^2 f_2}{\partial I \partial S} = 0, \frac{\partial^2 f_2}{\partial I^2} = 2b - \frac{2\beta_h^* \mu_h}{A}, \frac{\partial^2 f_2}{\partial S \partial \beta_h} = 0, \frac{\partial^2 f_2}{\partial I \partial \beta_h} = 1.$$

Hence, we have

$$\begin{aligned} A &= v_2 \left(w_1 w_1 \frac{\partial^2 f_2}{\partial S^2} + w_1 w_2 \frac{\partial^2 f_2}{\partial S \partial I} + w_2 w_1 \frac{\partial^2 f_2}{\partial S \partial I} + w_2 w_2 \frac{\partial^2 f_2}{\partial I^2} \right) \\ &= 2 \frac{(A\mu_h b - (A\beta_v \mu_c + \mu_h^2(\mu_c + \mu_h + 1)))}{A\beta_v(\mu_h + \mu_c)}, \end{aligned}$$

and

$$\begin{aligned} B &= v_2 w_1 \frac{\partial^2 f_2}{\partial S \, \partial \beta_h} + v_2 w_2 \frac{\partial^2 f_2}{\partial I \, \partial \beta_h} \\ &= v_2 w_2. \end{aligned}$$

We can see that $B > 0$ without any condition and $A > 0$ if

$$b^\dagger = \frac{A\beta_v \mu_c + \mu_h^2(\mu_c + \mu_h + 1)}{A \, \mu_h}.$$

Hence, system (4) undergoes a backward bifurcation at $R_0 = 1$ if $b^\dagger = \frac{A\beta_v \mu_c + \mu_h^2(\mu_c + \mu_h + 1)}{A \, \mu_h}$. Hence, the proof is complete. ■

Recall that b is the saturation parameter for the treatment. Therefore, we have the following remark.

Remark 2. *A more significant saturation parameter (indicated by lack of facility of treatment, the minimum number of beds in the hospital, minimum number of doctors, and other treatment facilities) will increase the probability of the existence of endemic equilibrium state of COVID-19, even though the disease-free state is stable when* $R_0 < 1$.

2.1.3 Numerical experiments

In this section, we illustrate the numerical examples of the possible phenomena of the COVID-19 model in (4), especially describing Theorem 2 numerically.

Example 1. Forward bifurcation. From Section 3, we found that system (4) will have a forward bifurcation whenever $b < b^{\dagger}$. To illustrate this phenomenon, we use the following parameters:

$$\beta_h^* = \frac{1000}{65 \times 365} \times 6, \beta_v^* = 10^{-10} \times \frac{10^3}{5} \times 6, \mu_h^* = \frac{1}{65 \times 365} \times 6, \mu_c^* = 10^{-4}.$$

Using this parameter, we found that $b^{\dagger} = 10^{-3}$. Therefore, to conduct the forward bifurcation, we choose $b = 10^{-4} < b^{\dagger}$. A bifurcation diagram for system (4) is shown in Fig.1 with respect to β_h as the bifurcation parameter. In this setting, we found that system (4) only has the COVID-19 free equilibrium as the stable equilibrium whenever $\beta_h^* < 1.0023$ ($R_{0(\beta_h=1.0023)} = 1$). When β_h^* increases, leaving $\beta_h^* = 1.0023$, the COVID-19-free state becomes unstable. On the other hand, the stable COVID-19 endemic starts to appear and increases when β_h^* increases. Biologically, this means that system (4) is robust with the initial condition as the long-term behavior of the model only depends on R_0 whether its larger or smaller than 1.

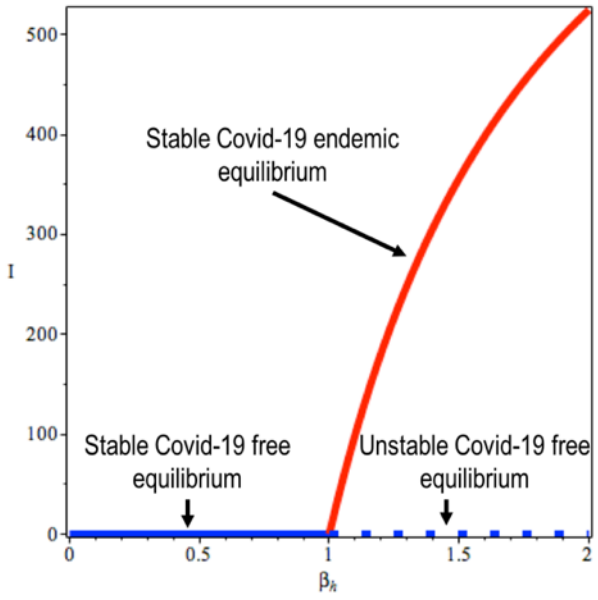

FIGURE 1**.** A forward bifurcation phenomenon of system (4) appears when $b < b^{\dagger}$. The blue and red curve indicates a COVID-19-free state and COVID-19 endemic state, respectively. Dotted and solid curves indicate unstable and stable states, respectively.

Example 2. Backward bifurcation. Similar to the previous example, from Section 3 we found that system (4) will have a backward bifurcation whenever $b > b^{\dagger}$. To illustrate this phenomenon, we use the same parameter value as example 1. Therefore, to conduct the backward bifurcation, we choose $b = 10^{-2} > b^{\dagger}$. A bifurcation diagram for system (4) shows in Fig.2 with respect to β_h^* as the bifurcation parameter. In this setting, we found that system (4) only has the COVID-19 free equilibrium as the stable equilibrium whenever $\beta_h^* < 0.385$. When $\beta_h^* = 0.385$, ***hysteresis*** appears, which is shown by the appearance of another positive equilibrium. Furthermore, when β_h^* increases from 0.385 until 1.0023, system (4) generates one stable COVID-19 endemic state and one unstable COVID-19 endemic state. On the other hand, the COVID-19-free equilibrium remains stable in this region. Therefore, a ***bistability*** phenomenon appears in this region. When β_h^* increases, leaving $\beta_h^* = 1.0023$, R_0 becomes larger than unity. Consequently, there is only one stable state, i.e. the COVID-19 endemic state, while the COVID-19 free state becomes unstable. Biologically, this implies that system (4) is very sensitive to a small perturbation in the initial condition whenever backward bifurcation occurs as it might lead to a large difference in the dynamic behavior of COVID-19 final state.

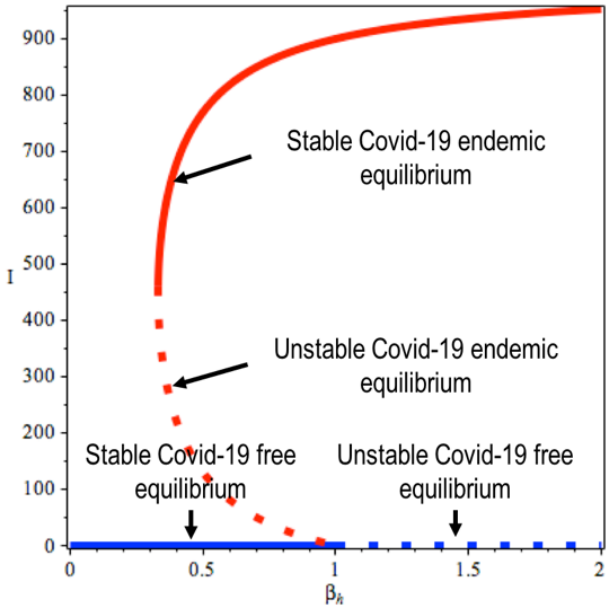

FIGURE 2. A backward bifurcation phenomenon of system (4) appear when $b > b^{\dagger}$. The blue and red curves indicate COVID-19 free state and COVID-19 endemic state, respectively. The dotted and solid curves indicate unstable and stable states.

2.1.4 Preliminary conclusions

In this section, we propose an epidemic model with a saturation recovery rate from infected to susceptible population considering the indirect transmission from the free pathogen. Our mathematical analysis started by approximating the coronavirus compartment in its equilibrium condition using the QSSA approach. Our model has two equilibrium states. The COVID-19 free state is locally stable if the basic reproduction number is less than one and becomes unstable otherwise. Our analysis shows that it is possible that the COVID-19 endemic state might appear even if the basic reproduction number is less than unity. This condition might lead to a misinterpretation of the condition of the COVID-19 eradication program by the policymaker in the community. Our analysis also shows that the indirect transmission which occurs from touching objects that contain viruses on their surface could increase the possibility of the existence of COVID-19 in the community. Therefore, except only using social/physical distancing and rapid assessment [21] or medical treatment [22], the use of disinfectant to wipe out the coronavirus that could potentially cause indirect transmission could be considered an additional effort to reduce COVID-19 transmission. Hence, we will **improve** our proposed model to consider three different interventions: medical mask use, disinfectant, and treatment. These three interventions will be introduced as a time-dependent parameter in the following section.

2.2 Improved model with control program

Based on our previous analysis, it is important to consider other interventions except focusing on social distancing to eradicate COVID-19. Hence, in this section, we modify our previous COVID-19 transmission model in (1). The modification entails adding three different interventions with specific purposes; they are as follows:

(i) **Medical mask.** The medical mask is strongly recommended by many policymakers in many countries not only for the infected individual but also for the susceptible one as many infected people do not show any symptoms. In our model, this intervention is denoted by $u_1(t)$. The construction of the model is as follows. First, we assume that only $u_1(t)$ proportion of the human population use a medical mask, while the rest $(1 - u_1(t))$ do not. Furthermore, we assume that the use of a medical mask could protect

humans from direct contact with infected individuals perfectly with the efficacy of the medical mask being 100%. Therefore, the infection caused by contact with an infected individual is 0. Hence, infection from direct contact only occurs from contact between a susceptible and an infected individual who does not wear any medical mask, i.e. (1-$u_1(t)$)$S(t)$ and (1-$u_1(t)$)$I(t)$, respectively. Therefore, the new infection coming from direct contact with an infected individual is given as follows:

$$\Lambda_h(t) = \frac{\beta_h\big(1-u_1(t)\big)S\,(1-u_1(t))I}{S+I} = \frac{\beta_h(1-u_1(t))^2SI}{S+I}.$$

(ii) **Disinfectants**. Disinfectants are implemented to kill coronavirus, which probably lies in the surface that already touch/had droplet by an infected individual previously. In our model, we denote this intervention as $u_2(t)$.

(iii) **Treatment**. Although specific medicine to cure infected individuals has not yet been created, medical support can still increase the recovery rate of an infected individual. We use $u_3(t)$ to symbolize this intervention on our model.

Considering these kinds of interventions, the COVID-19 transmission model in this article can be read as follows:

$$\begin{aligned}
\frac{dS}{dt} &= A - \frac{\beta_h(1-u_1(t))^2SI}{S+I} - \beta_v S\,V - \mu_h S + \frac{(\alpha + u_3(t))I}{1+bI},\\
\frac{dI}{dt} &= \frac{\beta_h(1-u_1(t))^2SI}{S+I} + \beta_v S\,V - \mu_h I - \frac{(\alpha + u_3(t))I}{1+bI} - \mu_c I,\\
\frac{dV}{dt} &= \xi I - (\mu_v + u_2(t))V,
\end{aligned} \tag{6}$$

which is supplemented with the following initial condition:

$$S(t=0) = S_0 \geq 0, I(t=0) = I_0 \geq 0, V(t=0) = V_0 \geq 0.$$

2.2.1 The basic reproduction number

Assuming all interventions are constant in time, system (6) has a COVID-19 free equilibrium given by

$$\Gamma_0 = (S, I, V) = \left(\frac{A}{\mu_h}, 0, 0\right). \tag{7}$$

Using the next-generation matrix method [16], the basic reproduction number of system (6) is given by

$$R_0^{intervention} = R_d + R_i = \frac{\beta_h(1-u_1)^2}{(\mu_h+\mu_c+\alpha+u_3)} + \frac{\beta_v A\xi}{\mu_h(\mu_v+u_2)(\mu_h+\mu_c+\alpha+u_3)}. \quad (8)$$

Please note that R_d denotes the basic reproduction number for the direct transmission caused by contact between the susceptible and the infected individual, while R_i is the infection from the indirect infection. From [24] we have the following theorem.

Theorem 4. *The COVID-19 free equilibrium Γ_0 of system (6) is locally asymptotically stable if $R_0 < 1$ and unstable otherwise.*

2.2.2 Characterization of the optimal control problem

In this section, we analyze the optimal control problem for COVID-19 transmission model (6) to determine the optimal trajectories of $S(t), I(t),$ and $V(t)$ which correspond to the optimal intervention strategy. Let us define the objective function as follows:

$$J(u_1,u_2,u_3) = \int_0^{t_f} \left(b_1 I(t) + b_2 V(t) + \frac{1}{2}c_1u_1^2 + \frac{1}{2}c_2u_2^2 + \frac{1}{2}c_3u_3^2 \right) dt. \quad (9)$$

This objective function describes the aim of our optimal control problem: minimizing the number of infected people and free coronavirus in the environment with a minimum cost of intervention strategies. We assume that the cost of the treatment is quadratic as has already been used by many authors in [12, 17, 20, 24]. The positive coefficients $b_1, b_2, c_1, c_2,$ and c_3 are the weight parameters which will guarantee the balance of each component in the cost function (9).

The Pontryagin Maximum Principle [25] has been used in this article to derive the necessary conditions that the optimal control parameters should satisfy. According to this principle, $u_1^*, u_2^*,$ and u_3^* as the optimal trajectories of control parameters with corresponding optimal $S^*, I^*,$ and V^* will minimize the cost function $J(u_1,u_2,u_3)$ for a fixed final time t_f.

(i) *The optimality condition*

$$\frac{\partial H(S,I,V,u_1,u_2,u_3,Z)}{\partial u_1} = 0,$$
$$\frac{\partial H(S,I,V,u_1,u_2,u_3,Z)}{\partial u_2} = 0, \frac{\partial H(S,I,V,u_1,u_2,u_3,Z)}{\partial u_3} = 0, \quad (10)$$

where $Z = \{z_s, z_i, z_v\}$ is the co-state variables and the Hamiltonian function $H(S,I,V,u_1,u_2,u_3,Z)$ is defined by

$$H = b_1 I(t) + b_2 V(t) + \frac{1}{2}c_1u_1^2 + \frac{1}{2}c_2u_2^2 + \frac{1}{2}c_3u_3^2 \quad (11)$$

$$+ z_s\left(A - \frac{\beta_h\left(1-u_1(t)\right)^2 SI}{S+I} - \beta_v S\,V - \mu_h S + \frac{\left(\alpha + u_3(t)\right)I}{1+bI}\right)$$

$$+ z_i\left(\frac{p\beta_h\left(1-u_1(t)\right)^2 SI}{S+I} + \beta_v S\,V - \mu_h I - \frac{\left(\alpha + u_3(t)\right)I}{1+bI} - \mu_c I\right)$$

$$+ z_v(\xi I - (\mu_v + u_2(t))V).$$

(ii) The co-state system

$$\frac{dz_s}{dt} = -\frac{\partial H}{\partial S}, \quad \frac{dz_i}{dt} = -\frac{\partial H}{\partial I}, \quad \frac{dz_v}{dt} = -\frac{\partial H}{\partial V} \tag{12}$$

(iii) *The optimal control system*

$$\frac{dS}{dt} = -\frac{\partial H}{\partial z_s}, \quad \frac{dI}{dt} = -\frac{\partial H}{\partial z_i}, \quad \frac{dV}{dt} = -\frac{\partial H}{\partial z_v} \tag{13}$$

(iv) *The minimization conditions*

$$H(S^*, I^*, V^*, u_1^*, u_2^*, u_3^*, Z^*) = \min_{0 \le u_i \le 1} H(S, I, V, u_1, u_2, u_3, Z) \tag{14}$$

is true for all $t \in [0, t_f]$.

(v) *The transversality conditions are true*

$$z_s(t_f) = 0, \quad z_i(t_f) = 0, \quad z_v(t_f) = 0. \tag{15}$$

Theorem 5. *Given the optimal controls* (u_1^*, u_2^*, u_3^*) *and corresponding state trajectories* (S^*, I^*, V^*) *of system (6), there exist the co-state variables which satisfy*

$$\frac{dz_s}{dt} = \frac{\beta_h I}{S+I}\left((1-u_1)^2 - \frac{(1-u_1)^2 S}{S+I} + \beta_v V\right)(z_s - z_i) + \mu_h z_s,$$

$$\frac{dz_i}{dt} = -b_1 + \left[\frac{(1-u_1)^2\beta_h S}{S+I}\left(1 - \frac{I}{S+I}\right) + \frac{\alpha + u_3}{1+bI}\left(\frac{bI}{1+bI} - 1\right)\right](z_i - z_s) \ldots \tag{16}$$

$$+ (\mu_h + \mu_c)z_i - \xi z_v,$$

$$\frac{dz_v}{dt} = -b_2 + \beta_v S\,(z_s - z_i) + (\mu_v + u_2)z_v,$$

supplemented with $z_s(t_f) = 0, \quad z_i(t_f) = 0, \quad z_v(t_f) = 0$. *Furthermore,*

$$u_1^*(t) = \min\left\{\max\left\{\frac{2SI\beta_h(z_i - z_s)}{2SI\beta_h(z_i - z_s) + c_1(S+I)}, 0\right\}, 0.1\right\},$$
$$u_2^*(t) = \min\left\{\max\left\{\frac{z_v V}{c_2}, 0\right\}, 0.1\right\}, \quad (17)$$
$$u_3^*(t) = \min\left\{\max\left\{\frac{I(z_i - z_s)}{c_3(1+bI)}, 0\right\}, 0.1\right\}.$$

Proof. The co-state system in (16) is the direct result from equation (12) in which we differentiate the Hamiltonian H with respect to each state variable. The transversality condition is derived from (15). Taking the derivative of H with respect to u_1, solving it with respect to zero, and combining it with its lower bound and upper bound 0 and 1 respectively, we have $u_1^*(t)$ in equation (17). A similar approach is used to find u_2^* and u_3^*. ■

3. RESULTS IN THE OPTIMAL CONTROL PROBLEM

To conduct the numerical simulation for the optimal control problem in this article, we use the so-called forward-backward iterative method [26] and MATLAB codes for the implementation. Please see [12, 17, 20, 24, 28-30] for other examples for the implementation of this method.

Generally, the forward-backward iterative method is as follows. We begin with having an initial estimation for all control variables, solving the state variables in system (6) forward in time for all time $t \in [0, t_f]$, and then calculating the value of initial cost function (9). Having the solutions of all state variables, we use the same to find the solution to all co-state variables using system (16) backward in time. We update our control variables using (17). Using these updated control variables, we re-calculate the state variables and cost function. We repeat this step until some convergence condition is achieved, which in this case is that the norm-2 difference of control and state variables in iteration $k+1$ compared to the k^{th} iteration should be less than small number ϵ.

To conduct the simulation in this section, we use the following parameter values:

$$A = \frac{100000}{65 \times 365}, \beta_h = 0.4, \beta_v = 8 \times 10^{-11}, \alpha = \frac{1}{2},$$
$$\mu_h = \frac{1}{65 \times 365}, b = \frac{1}{10000}, \mu_c = \frac{3}{100}, \xi = 10000, \mu_v = \frac{1}{2},$$

and all controls are 0. These parameter values give us $R_0 = 1.06$. Since $R_0 > 1$, the disease-free equilibrium point becomes unstable and it exists in a stable endemic equilibrium state, i.e.

$$S = 80509, \quad I = 28, \quad V = 5.5 \times 10^9.$$

In simulating the optimal control problem, we use three different strategies, i.e. the use of single intervention (Section 3.1), two interventions (Section 3.2), and all interventions (Section

3.3). To run the optimal control simulation, we use the aforementioned parameter value, weight parameter as follows

$$b_1 = 1, b_2 = 1, c_1 = 10^{12}, c_2 = 10^{12}, c_3 = 10^{17},$$

to balance the cost function and describe the cost for implementation. It is evident that $c_1 = c_2$ as the cost for medical mask use is almost the same as the cost for personal disinfectant use. On the other hand, c_3 is higher than c_1 and c_2 as the cost for medical intervention requires a more expensive cost for implementation. Furthermore, we use the following state initial condition:

$$(S_0, I_0, V_0) = (99.000, 1.000, 0).$$

3.1 Single intervention

It can be seen from Fig. 3–5 that without the implementation of any control, the dynamic of infected peoples increased to outbreak at Day 40 and started decreasing to equilibrium when t started increasing. Consequently, the implementation of control will behave related to the dynamic of the infected individual. It can be seen that u_1 and u_2 are maximum from the beginning of the simulation time until a few days after the outbreak; they then start to decrease to 0. On the other hand, the dynamic of u_3 is monotonically decreasing from the beginning of simulation time. This is probably because the cost of treatment in the hospital is high compared to other interventions.

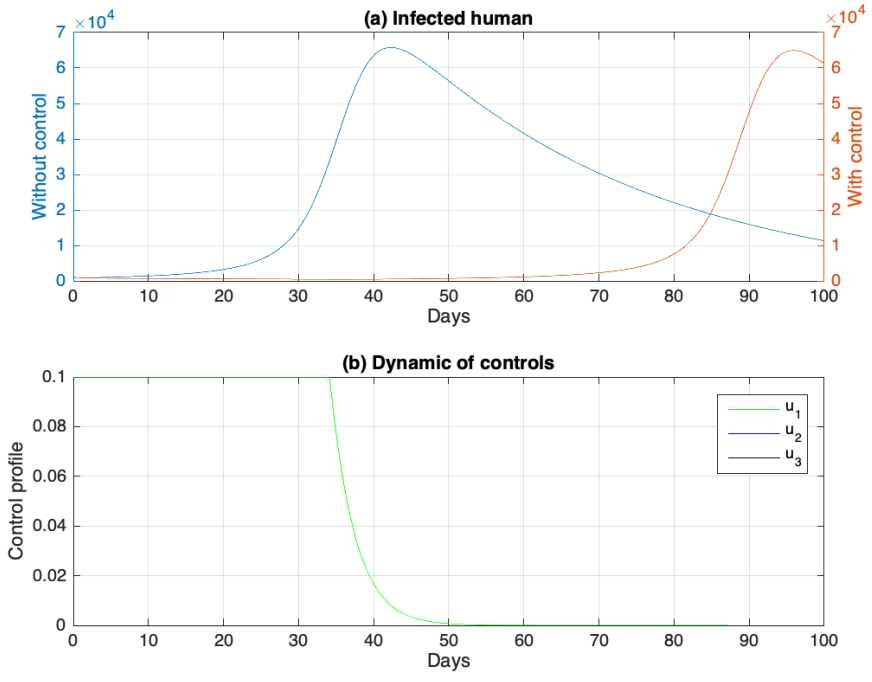

FIGURE 3. Dynamic of infected individual and control profile for Strategy 1: Medical mask use only.

3.2 Combination of two interventions

In Fig. 6, we can see that each strategy could reduce the number of predicted infected individuals with a combination of $u_1$and u_2 to yield a better result (please see the green curve in Fig. 6) with the cost function $J = 6.844 \times 10^{11}$. Second-best interventions are provided by a combination of u_1 and u_3 (please see the blue curve in Fig. 7) with the cost function $J = 3.945 \times 10^{14}$. Compared to $u_1$and u_2 only, the number of infected individuals increases in the time close to the final time of simulation which indicates that possible delayed outbreak will occur. From 8, a combination of u_2 and u_3 should be given at a maximum rate at the beginning of the simulation and start to decrease when the peak of the outbreak passes.

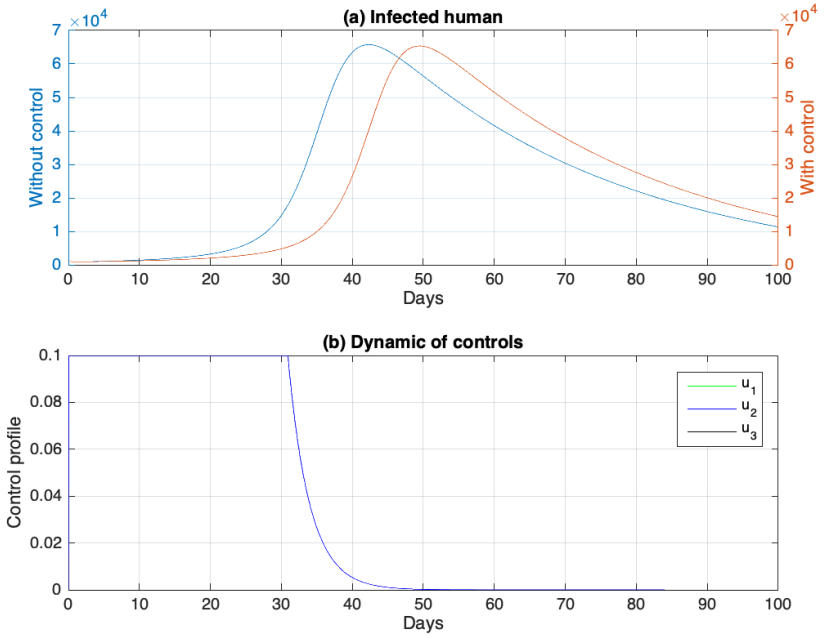

FIGURE 4. Dynamic of infected individual and control profile for Strategy 2: disinfectant use only.

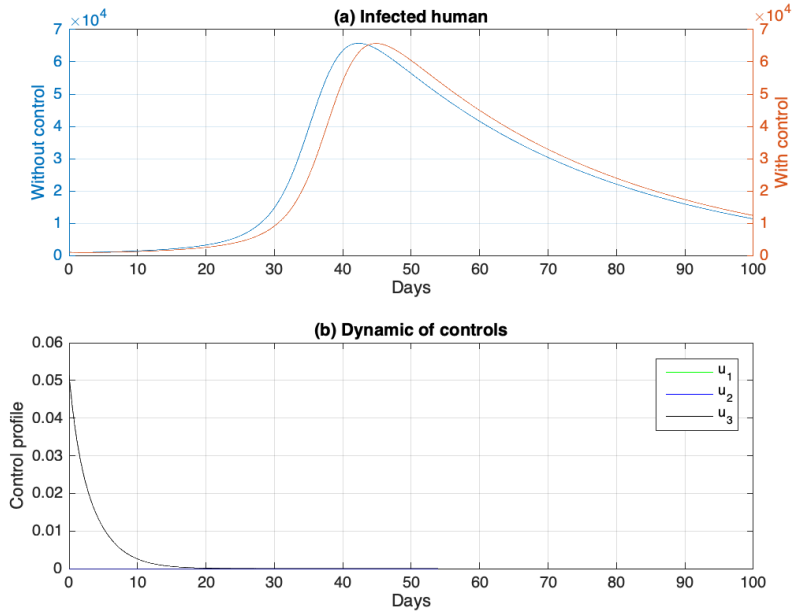

Figure 5. Dynamic of infected individual and control profile for Strategy 3: medical treatment only.

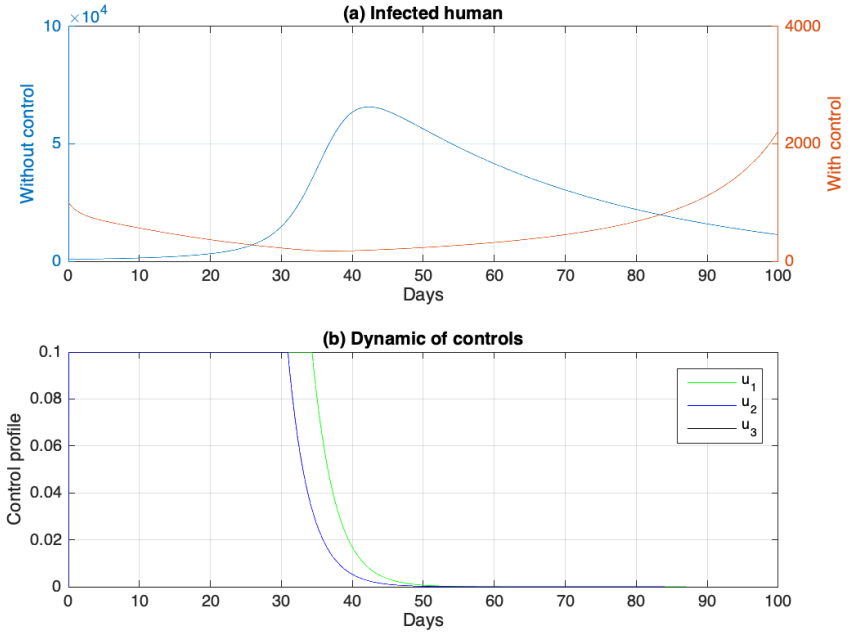

FIGURE 6. Dynamic of infected individual and control profile by combining two controls for Strategy 4: medical mask and disinfectant use

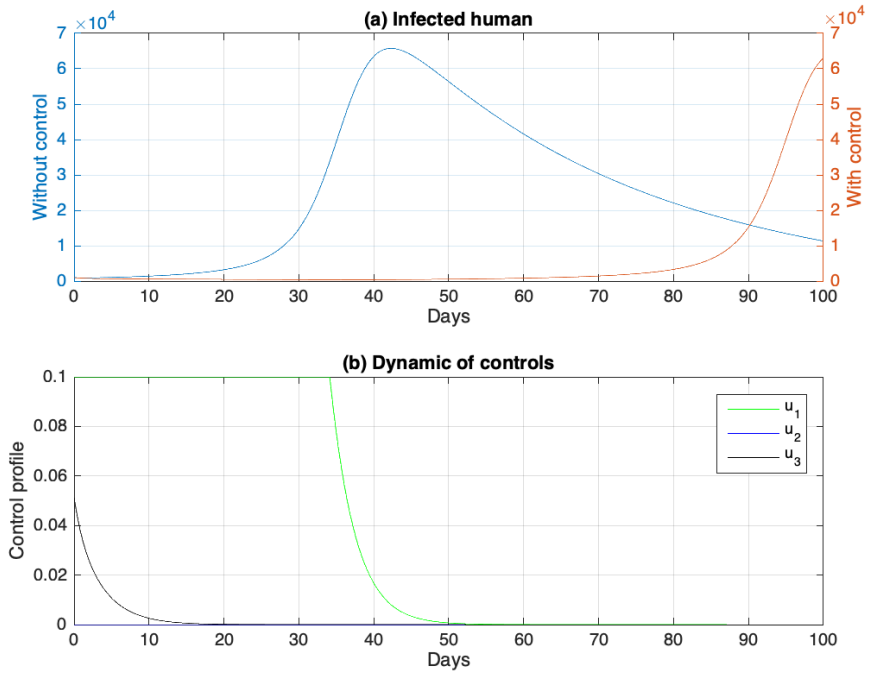

FIGURE 7. Dynamic of infected individual and control profile by combining two controls for Strategy 5: medical mask and treatment use.

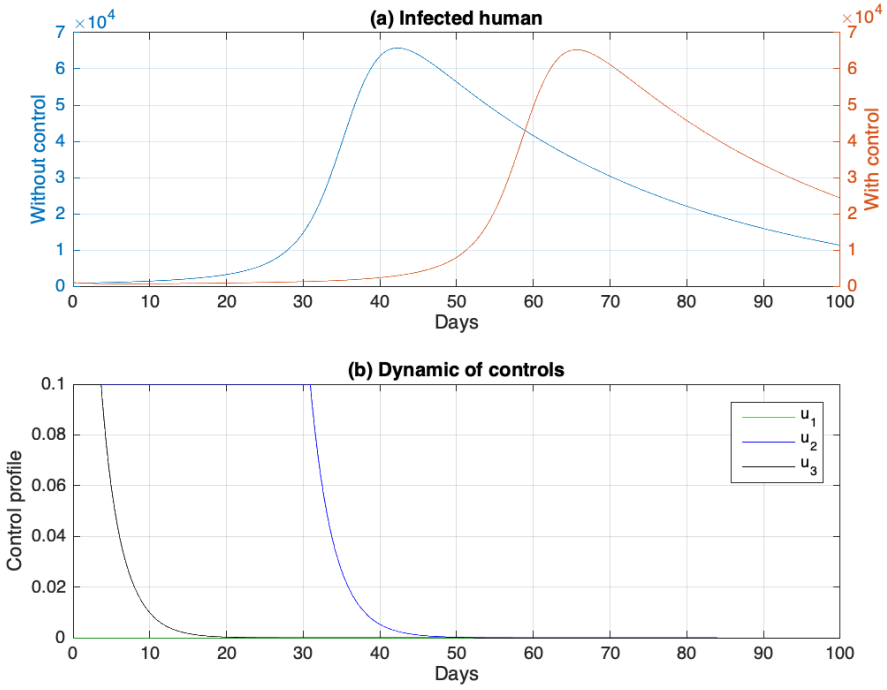

FIGURE 8. Dynamic of infected individual and control profile by combining two controls for Strategy 6: disinfectant and medical treatment.

3.3 Combination of all interventions

From Fig.9, it is evident that the number of infected individuals can be reduced significantly from the beginning of simulation time to be less than 1000 individuals for the entire simulation. For the control interventions, it can also be seen that they are only present at a high rate before the predicted outbreak (without control strategy) occurs; all controls start to decrease to 0 after that. It is also apparent that u_1 maintains the highest rate longer than other controls. The cost for intervention when all interventions are in place is 4.9×10^{13}.

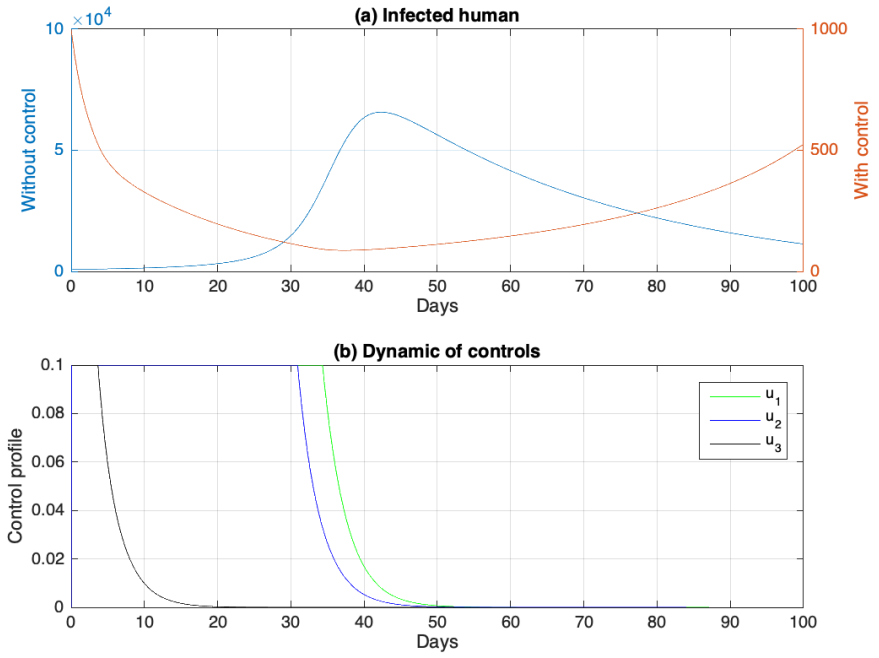

FIGURE 9. Dynamic of infected human (a) and controls (b) when all interventions are combined in a single implementation (Strategy 7).

4. Cost-Effectiveness Analysis

In this section, we perform a cost-effectiveness analysis of our optimal control Strategy discussed in Section 3. We consider two types of methods to determine the best strategies, namely the infection averted ratio (IAR) approach and the average cost-effectiveness ratio (ACER) approach. The IAR is defined as

$$IAR = \frac{\text{number of infection averted}}{\text{Number of recovered}}.$$

The highest IAR ratio is the best strategy. On the other hand,

$$ACER = \frac{\text{Total cost produced by intervention}}{\text{Total number of infection averted}}.$$

The smallest value of ACER is the best strategy. The result for numerical calculation according to total cost function (9), number of infected averted, total recovery, cost for intervention, IAR and ACER can be seen in Table 1.

No	Strategy	J in Eq (9)	Infected averted	Total recovered	Cost for intervention	IAR	ACER
1	$u_1 \neq 0, u_2 = 0, u_3 = 0$	$3{,}74 \times 10^{11}$	$3{,}23 \times 10^{7}$	$2{,}29 \times 10^{6}$	$7{,}16 \times 10^{12}$	14,123	$2{,}212 \times 10^{5}$
2	$u_1 = 0, u_2 \neq 0, u_3 = 0$	$3{,}725 \times 10^{11}$	$1{,}78 \times 10^{6}$	$5{,}56 \times 10^{6}$	$6{,}48 \times 10^{12}$	0,323	$3{,}63 \times 10^{6}$
3	$u_1 = 0, u_2 = 0, u_3 \neq 0$	$3{,}94 \times 10^{14}$	$5{,}98 \times 10^{5}$	$5{,}73 \times 10^{6}$	$7{,}88 \times 10^{15}$	0,104	$1{,}318 \times 10^{10}$
4	$u_1 \neq 0, u_2 \neq 0, u_3 = 0$	$6{,}844 \times 10^{11}$	$4{,}99 \times 10^{7}$	$5{,}08 \times 10^{5}$	$1{,}36 \times 10^{13}$	98,19	$2{,}73 \times 10^{5}$
5	$u_1 \neq 0, u_2 = 0, u_3 \neq 0$	$3{,}945 \times 10^{14}$	$4{,}03 \times 10^{7}$	$1{,}747 \times 10^{6}$	$7{,}89 \times 10^{15}$	23,07	$1{,}957 \times 10^{8}$
6	$u_1 = 0, u_2 \neq 0, u_3 \neq 0$	$4{,}965 \times 10^{15}$	$7{,}9 \times 10^{6}$	$4{,}569 \times 10^{6}$	$9{,}929 \times 10^{16}$	1,729	$1{,}257 \times 10^{10}$
7	$u_1 \neq 0, u_2 \neq 0, u_3 \neq 0$	$4{,}965 \times 10^{15}$	$5{,}054 \times 10^{7}$	$2{,}31 \times 10^{5}$	$9{,}93 \times 10^{16}$	218,74	$1{,}965 \times 10^{9}$

Table 1. Numerical result for optimal control Strategy in Section 3.

4.1 Infected averted ratio (IAR)

According to Fig. 9, the best strategy is Strategy 7 when all controls are implemented. The second and third best are Strategy 4 (when medical mask and disinfectant combined) and Strategy 5 (when the medical mask and medical treatment are combined), respectively. We can see that Strategy 3 is the least cost-effective.

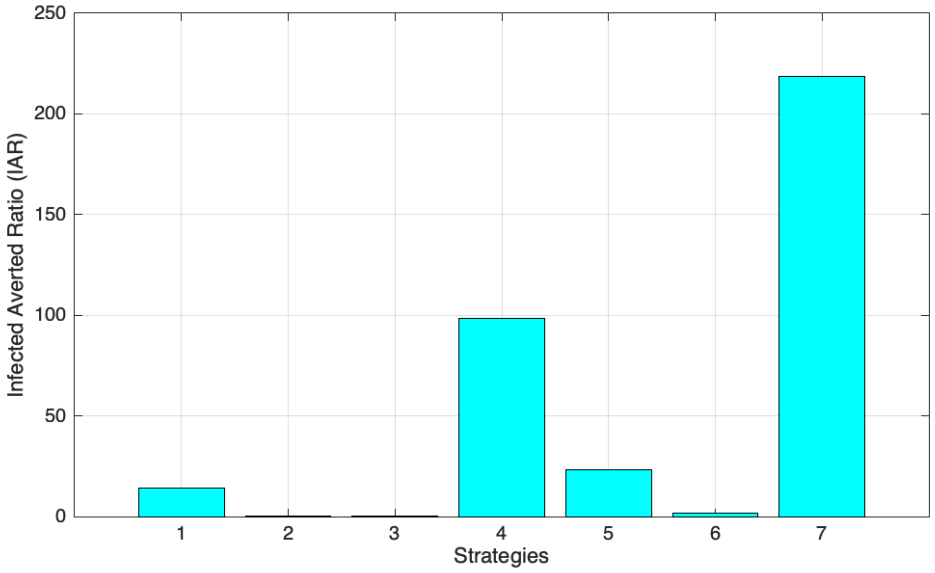

FIGURE 10. IAR plots indicating the effect of the seven strategies that were conducted in Sec.3.

4.2 Average cost-effectiveness ratio (ACER)

Fig. 10 shows that the three most effective strategies are Strategies 1, 4, and 2, respectively (magenta bar). On the other hand, Strategies 5, 7, 6, and 3 are the least effective, respectively (red bar). This result indicates that the single strategy of using a medical mask only is the best single strategy if there is a budget limitation for the eradication of COVID-19.

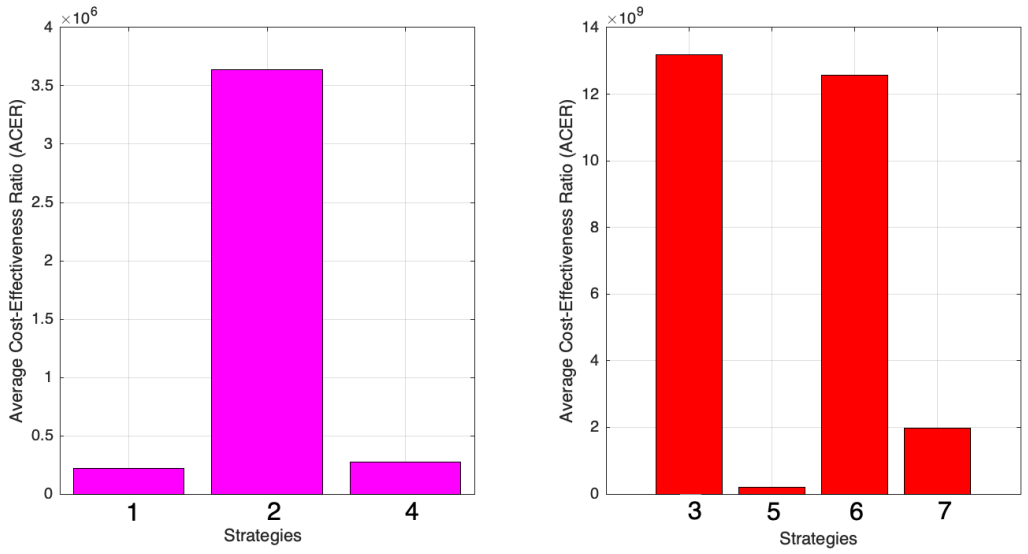

FIGURE 11. ACER plots indicating the effect of the seven strategies that were analyzed in Sec.3.

5. DISCUSSION AND CONCLUDING REMARKS

In this study, a deterministic model for understanding the spread of COVID-19 that considers direct and indirect transmission has been proposed as a system of ordinary differential equations. Mathematical analysis of the existence and local stability criteria of all equilibrium points was conducted and indicated how the basic reproduction number plays an important role in determining the long-term behavior of the model. Our proposed model might exhibit a backward bifurcation phenomenon at $R_0 = 1$ if the saturated treatment parameter is larger than its threshold.

Further improvement of the model under the interventions medical mask, disinfectant, and medical treatment were proposed later. The model has a disease-free equilibrium which is locally stable when the basic reproduction number is less than one. The optimal control problem of the proposed model constructed is based on Pontryagin's Maximum Principle to minimize the number of infected individuals with an optimal cost. The problem was solved using the forward-backward iterative method.

The numerical simulation of the optimal control problem was conducted using three strategies. In the first Strategy, when only a single intervention was implemented, our simulation revealed that the medical mask use is the best single intervention strategy. This was followed by disinfectant and medical treatment. In the second Strategy, a combination of medical mask use and disinfectant yielded a better result compared to the other combination. In the last Strategy, a combination of all

interventions together provided the best result in reducing the number of infected individuals compared to the best strategy in the first and second strategies. All strategies show the profile of control adapted with the number of infected individuals in the community. A larger intervention is needed to substantially reduce the number of infected individuals, and this intervention then start to reduce whenever the number of infected individual start to show a trend to decrease. Further analysis to determine the most cost-effective strategy was conducted using the IAR and ACER indices. We found that using all controls simultaneously is the most cost-effective method based on the calculation of IAR and that using a medical mask only is the most cost-effective method in a single intervention which was analyzed using the ACER calculations.

The results in this study provide an alternative scientific background for the eradication of COVID-19 in the community. The limitation of budget that will force policymakers to save on intervention costs by choosing priority strategies has been discussed here. Each intervention has its own focus. If the policy is to reduce the number of deaths, then the intervention should focus on medical treatment. However, this intervention comes with high-cost consequences. On the other hand, if the policy is to prevent the outbreak of COVID-19, then medical mask use or disinfectant intervention or combination of both is the best strategy as that could prevent the outbreak well. It also costs less compared to medical treatment intervention. For future work, including other interventions into the model could be considered such as physical/social distancing intervention, rapid infected assessment, quarantine, and many more.

ACKNOWLEDGMENTS

This research is financially supported by the Ministry of Research, Technology and Higher Education of the Republic of Indonesia (Kemenristek DIKTI) with the PUPT research grant scheme 2020 (ID Number: NKB-2803/UN2.RST/HKP.05.00/2020).

CONFLICT OF INTERESTS

The authors declare that there is no conflict of interests.

REFERENCES

[1] WHO. Coronavirus disease 2019 (COVID-19). Situation report 24. February 13, 2020. Geneva: World Health Organization, 2020.

[2] www3.nhk.or.jp. Accessed on April 17, 2020.

[3] N. Ferguson, D. Laydon, G. Nedjati Gilani, et al. Report 9: Impact of non-pharmaceutical interventions (NPIs) to reduce COVID19 mortality and healthcare demand, Imperial College London, 2020. https://doi.org/10.25561/77482.

[4] D. Aldila, S.H.A. Khoshnaw, E. Safitri, et al. A mathematical study on the spread of COVID-19 considering social distancing and rapid assessment: The case of Jakarta, Indonesia, Chaos Solitons Fractals. 139 (2020), 110042.

[5] Z. Liu, P. Magal, O. Seydi, G. Webb, Understanding Unreported Cases in the COVID-19 Epidemic Outbreak in Wuhan, China, and the Importance of Major Public Health Interventions, Biology. 9 (2020), 50.

[6] B. Tang, X. Wang, Q. Li, et al. Estimation of the Transmission Risk of 2019-nCov and Its Implication for Public Health Interventions. J. Clin. Med. 9 (2020), 462.

[7] N. Nuraini, K. Khairuddin, M. Apri, Modeling Simulation of COVID-19 in Indonesia based on Early Endemic Data, Commun. Biomath. Sci. 3 (1) 2020, 1-8.

[8] K. Roosa, Y. Lee, R. Luo, et al. Real-time forecasts of the COVID-19 epidemic in China from February 5th to February 24th, 2020, Infect. Dis. Model. 5 (2020), 256–263.

[9] G. Kampf, D. Todt, S. Pfaender, E. Steinmann, Persistence of coronaviruses on inanimate surfaces and their inactivation with biocidal agents, J. Hosp. Infect. 104 (2020), 246–251.

[10] J.A.M. Borghans, R.J. de Boer, L.A. Segel, Extending the quasi-steady state approximation by changing variables, Bull. Math. Biol. 58 (1996), 43–63.

[11] D. Aldila, S.L. Latifah, P.A. Dumbela, Dynamical analysis of mathematical model for Bovine Tuberculosis among human and cattle population, Commun. Biomath. Sci. 2 (1) (2019), 55-64.

[12] B.D. Handari, F. Vitra, R. Ahya, et al. Optimal control in a malaria model: intervention of fumigation and bed nets, Adv. Differ Equ. 2019 (2019), 497.

[13] B.D. Handari, A. Amalia, et al. Numerical simulation of malaria transmission model considering secondary infection, Commun. Math. Biol. Neurosci. 2020 (2020), 36.

[14] M.S. Khumaeroh, E. Soewono, N. Nuraini, A dynamical model of 'invisible wall' in mosquito control, Commun. Biomath. Sci. 1 (2) (2018), 88-99.

[15] D. Aldila, H. Seno, A Population Dynamics Model of Mosquito-Borne Disease Transmission, Focusing on Mosquitoes' Biased Distribution and Mosquito Repellent Use, Bull. Math. Biol. 81 (12) (2020), 4977-5008.

[16] O. Diekmann, J.A.P. Heesterbeek, M.G. Roberts, The construction of next-generation matrices for compartmental epidemic models, J. R. Soc. Interface, 7 (47) (2010), 873–885.

[17] D. Aldila, H. Padma, K. Khotimah, et al. Analyzing the MERS disease control strategy through an optimal control problem, Int. J. Appl. Math. Comput. Sci. 28 (1) (2018), 169-184.

[18] D. Aldila, N. Nuraini, E. Soewono, Optimal control problem in preventing of swine flu disease transmission, Appl. Math. Sci. 8 (71) (2014), 3501-3512.

[19] A. Bustamam, D. Aldila, A. Yuwanda, Understanding Dengue Control for Short- and Long-Term Intervention with a Mathematical Model Approach, J. Appl. Math. 2018 (2018),9674138.

[20] D. Aldila, B.D. Handari, A. Widyah, G. Hartanti, Strategies of optimal control for HIV spreads prevention with health campaign, Commun. Math. Biol. Neurosci. 2020 (2020), 7.

[21] M.Z. Ndii, P. Hadisoemarto, D. Agustian, A.K. Supriatna, An analysis of Covid-19 transmission in Indonesia and Saudi Arabia, Commun. Biomath. Sci. 3 (1) (2020), 19-27.

[22] Z. Yang, Z. Zeng, K. Wang, et al. Modified SEIR and AI prediction of the epidemics trend of COVID-19 in China under public health interventions, J. Thorac. Dis. 12 (2020), 165–174.

[23] P. van den Driessche, J. Watmough, Reproduction numbers and sub-threshold endemic equilibria for compartmental models of disease transmission, Math. Biosci. 180 (2002), 29–48.

[24] D. Gao, N. Huang, Optimal control analysis of a tuberculosis model, Appl. Math. Model. 58 (2018), 47–64.

[25] L.S. Pontryagin, V.G. Boltyanskii, R.V. Gamkrelidze, E.F. Mishchenko, The Mathematical Theory of Optimal Processes, Wiley, New York, 1962.

[26] S. Lenhart, J.T. Workman, Optimal Control Applied to Biological Models, in: Chapman & Hall/CRC Mathematical and Computational Biology Series, Chapman & Hall/CRC, Boca Raton, FL, 2007.

[27] C. Castillo-Chavez, B. Song, Dynamical models of tuberculosis and their applications. Math. Biosci. Eng. 1 (2) (2004), 361.

[28] S.I. Oke, M.M. Ojo, M.O. Adeniyi, M.B. Matadi, Mathematical modeling of malaria disease with control strategy, Commun. Math. Biol. Neurosci. 2020 (2020), 43.

[29] A. Kouidere, B. Khajji, A. El Bhih, O. Balatif, M. Rachik, A mathematical modeling with optimal control strategy of transmission of COVID-19 pandemic virus, Commun. Math. Biol. Neurosci. 2020 (2020), 24.

[30] H. Ferjouchia, F.Z. Iftahy, A. Chadli, et al. Application of optimal control strategies for physiological model of type 1 diabetes - T1D, Commun. Math. Biol. Neurosci. 2020 (2020), 35.